Cell Death and Differentiation (2007) 14, 1020–1028

www.nature.com/cdd

Failure of stress-induced downregulation of Bcl-2 contributes to apoptosis resistance in senescent human diploid fibroblasts

SJ Ryu[1], YS Oh[1] and SC Park*,[1]

We previously reported that senescent human diploid fibroblasts (HDFs) are resistant to apoptosis induced by H_2O_2 and staurosporine. We report here that senescent HDFs are resistant to thapsigargin-induced apoptosis as well. These agonists caused the reductions in mitochondrial membrane potential (MMP) and in the apoptosis inhibitory protein (B-cell lymphoma) only in young HDFs but not in senescent HDFs. In addition, downregulation of Bcl-2 increased the sensitivity of senescent HDFs to apoptosis induction, suggesting the significant role of Bcl-2 in apoptosis resistance of the senescent HDFs. We further found that P-cAMP response element-binding protein (CREB), a positive regulator of Bcl-2, decreased in stress-induced apoptosis of young HDFs but not in senescent HDFs, and that Bcl-2 was markedly reduced in CREB small interfering RNA (siRNA), transfected senescent HDFs. In addition, activity of protein phosphatase 2A (PP2A), which dephosphorylates p-CREB, significantly increased in young HDFs but not in senescent HDFs treated with H_2O_2, staurosporine or thapsigargin. Taken together, these results suggest that failure of stress-induced downregulation of Bcl-2 underlies resistance of senescent HDFs to apoptosis.
Cell Death and Differentiation (2007) **14,** 1020–1028. doi:10.1038/sj.cdd.4402091; published online 9 February 2007

The senescent phenotype is characterized by an increase in cell size, a distinct flat and enlarged morphology,[1,2] appearance of senescence-associated β-galactosidase (SA-β-galactosidase) activity,[3] hypo-responsiveness to growth factors,[4] resistance to apoptosis caused by stimuli such as UV, H_2O_2, staurosporine, etoposide and ceramide,[1,5,6] and broad changes in gene expression.[7] The mechanisms conferring resistance to stress-induced apoptosis in senescent human diploid fibroblasts have not been well studied.

The apoptosis inhibitory protein, Bcl-2 is the archetypal member of a family of genes that control programmed cell death, and play a vital role in determining the life span of many cell types.[8] There is a twofold increase in Bcl-2 in senescent HDFs compared with their young counterparts.[9] This higher level of Bcl-2 is suggested as a factor possibly contributing to the enduring survival of the senescent HDFs. As the underlying mechanism has not been clarified, we attempted to define the specific role of Bcl-2 in the development of resistance to apoptosis in senescent HDFs, using three different types of apoptotic stimuli: (1) H_2O_2, which induces reactive oxygen species (ROS) and causes caspase-3-dependent or independent apoptosis, depending on the cell type[10,11]; (2) staurosporine, a kinase inhibitor, which causes caspase-3-dependent apoptosis via a mitochondrial pathway[12]; and (3) thapsigargin, which disrupts ER Ca^{2+} stores, leading to Ca^{2+} release from the ER (endoplasmic reticulum), and unleashes mitochondrial-dependent as well as mitochondrial-independent (caspase-12-dependent) apoptotic pathways.[13] We found that when treated with H_2O_2, staurosporine or thapsigargin, Bcl-2 is markedly downregulated in young HDFs but not in senescent HDFs. Also, stress-induced apoptosis was enhanced in senescent HDFs when the expression of Bcl-2 gene was repressed, using a small interfering RNA (siRNA). Both these results suggest that regulation of Bcl-2 plays an important role in mediating the resistance to a variety of apoptotic stimuli in senescent HDFs. In studies designed to elucidate the regulatory mechanism for Bcl-2 expression, we found that Bcl-2 was markedly reduced in cAMP response element-binding protein (CREB) siRNA-transfected senescent HDFs and that the activity of protein phosphatase 2A (PP2A) (which is involved in the regulation of the transcriptional activities of CREB, a positive regulator of Bcl-2[14]) significantly increased in young HDFs treated with H_2O_2, staurosporine or thapsigargin but not in senescent HDFs. These findings confirm that downregulation of Bcl-2, which facilitates apoptosis in young HDFs, does not occur in senescent HDFs. This failure of downregulation of Bcl-2 in senescent cells is responsible for the resistance of these cells to stress-induced apoptosis.

Results

Senescent HDFs are resistant to thapsigargin-induced apoptosis. In a previous study, we reported that senescent HDFs showed apoptotic resistance toward H_2O_2 and

[1]Department of Biochemistry and Molecular Biology, The Aging and Apoptosis Research Center, Seoul National University College of Medicine, Seoul, Korea
*Corresponding author: SC Park, Department of Biochemistry and Molecular Biology, Aging and Apoptosis Research Center, Seoul National University College of Medicine, 28 Yungon Dong, Chong No Ku, Seoul 110-799, Republic of Korea. Tel: 82 2 740 8244; Fax: 82 2 744 4534; E-mail: scpark@snu.ac.kr
Keywords: apoptosis; senescence; fibroblast; Bcl-2; p-CREB; PP2A
Abbreviations: HDF, human diploid fibroblast; Bcl-2, B-cell lymphoma; SA-β Gal, senescence associated β-galactosidase; $DiOC_6$, 3,3′diethyloxacarbocyanine; MMP, mitochondrial membrane potential; FACS, fluorescence-activated cell sorter; PARP, poly(ADP-ribose)polymerase; siRNA, small interfering RNA; PP2A, protein phosphatase 2A; p-CREB, phospho-cyclic AMP response element-binding protein
Received 11.7.06; revised 28.11.06; accepted 29.11.06; Edited by C Borner; published online 09.2.07

staurosporine in contrast to young HDFs.[1] Employing 3-(4,5-dimethylthiazal-z-yl)-2,5-diphenylterazolium (MTT) assays, we show here that senescent HDFs, unlike the young HDFs, resist thapsigargin-induced apoptosis as well. The increased survival of senescent HDFs, relative to young HDFs under thapsigargin-induced stress, is shown in Figure 1a. After thapsigargin treatment for 48 h, subG_1/G_0 population significantly increased to 31.69% in young HDFs, whereas it did not change in senescent HDFs (Figure 1b and c). Also, caspase-3 and poly(ADP-ribose)polymerase (PARP) cleavage after thapsigargin treatment increased time dependently in young HDFs but not in the senescent HDFs (Figure 1d).

Changes of mitochondrial membrane potential ($\Delta\Psi_m$) in young and senescent HDFs. Dissipation of mitochondrial membrane potential ($\Delta\Psi_m$) has been detected during the early stage of the apoptotic process,[15] and $\Delta\Psi_m$ has been reported to decrease in aged cell.[16–18] We therefore compared the changes of $\Delta\Psi_m$ in young and senescent HDFs in response to H_2O_2, staurosporine and thapsigargin treatments by analyzing $DiOC_6$ fluorescence by flow cytometry. As shown in Figure 2, we observed that $\Delta\Psi_m$ of senescent HDFs decreased about two-fold compared with that of young HDFs, but dissipation of $\Delta\Psi_m$ was significantly increased in young HDFs but not in the senescent HDFs undergoing H_2O_2, staurosporine or thapsigargin-induced apoptosis.

Failure of stress-induced downregulation of Bcl-2 in senescent HDFs. The early events of apoptosis, including the reduction in $\Delta\Psi_m$, are regulated by proapoptotic proteins such as Bax[19] and antiapoptotic proteins such as Bcl-2 and Bcl-x_L.[20] The ratio of Bcl-2 to Bax following an apoptotic stimulus is believed to mainly determine whether a cell survives or dies.[21]

We monitored the expression levels of Bcl-2 family proteins in young and senescent HDFs before and after treatments

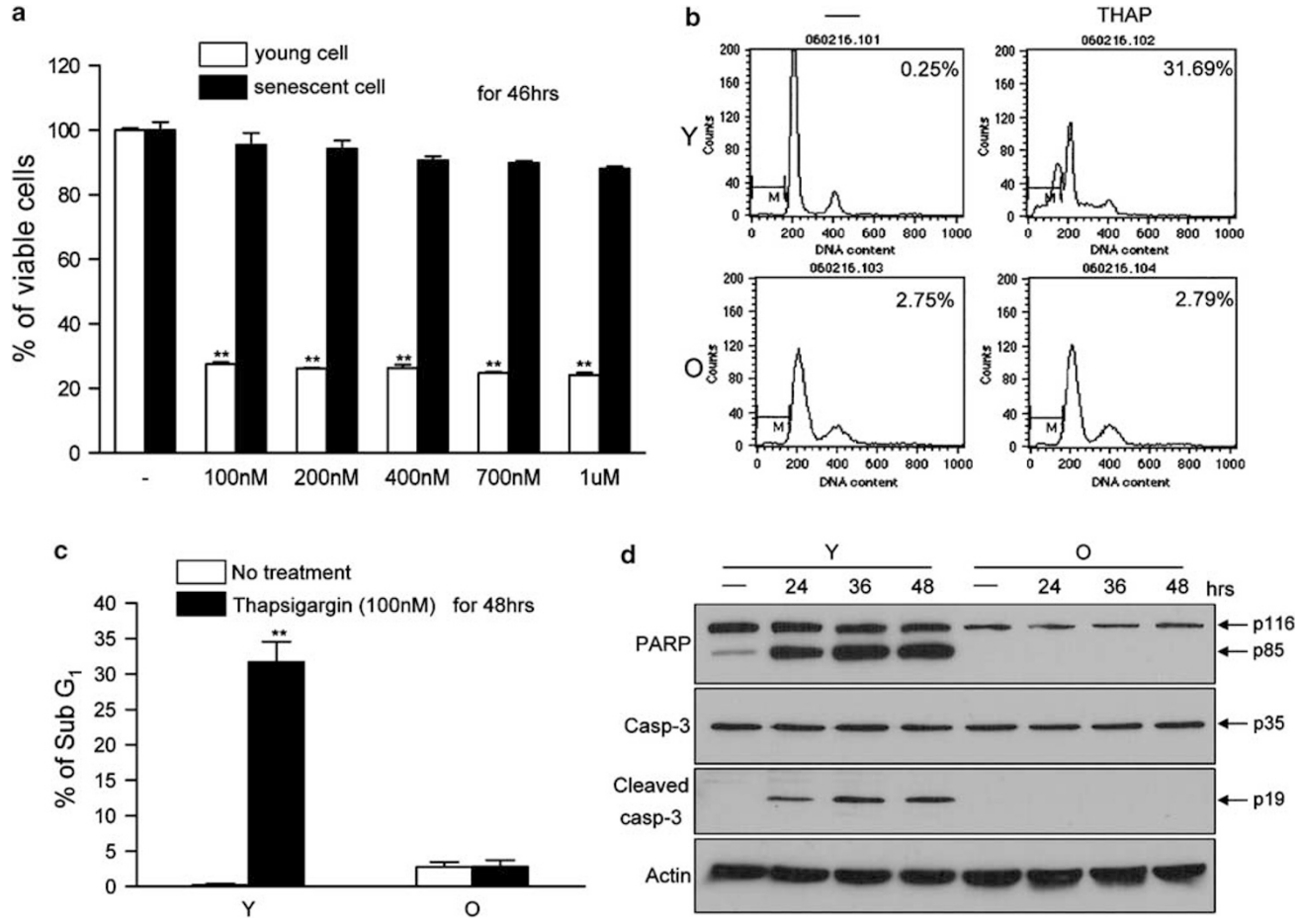

Figure 1 Senescent HDFs resist thapsigargin-induced apoptosis. (**a**) Following thapsigargin treatment, relative viabilities were determined by measuring absorbance or optical density at 490 nm (OD_{490}) in an MTT staining assay. Error bars represent standard deviations of the means. Significance was tested by ANOVA, Dunnett was used as post-test. $^{**}P<0.01$ *versus* the control group. (**b**) Young and senescent HDFs were treated with 100 nM thapsigargin for 48 h. Cells were stained with PI and determined by flow cytometry. (**c**) Quantitative graph of subG_1/G_0. The results shown are representative of three independent experiments; the histograms represent average and error bars represent standard deviations of the means. A double asterisk (**) denotes $P<0.01$ in a Student's *t*-test. (**d**) Young and senescent HDFs were treated with 100 nM thapsigargin for the indicated times, and cells were harvested. PARP cleavage and caspase-3 activation were analyzed by Western blotting using anti-PARP or anti-caspase-3 antibodies. Y, young HDF cells; O, senescent HDF cells; THAP, thapsigargin

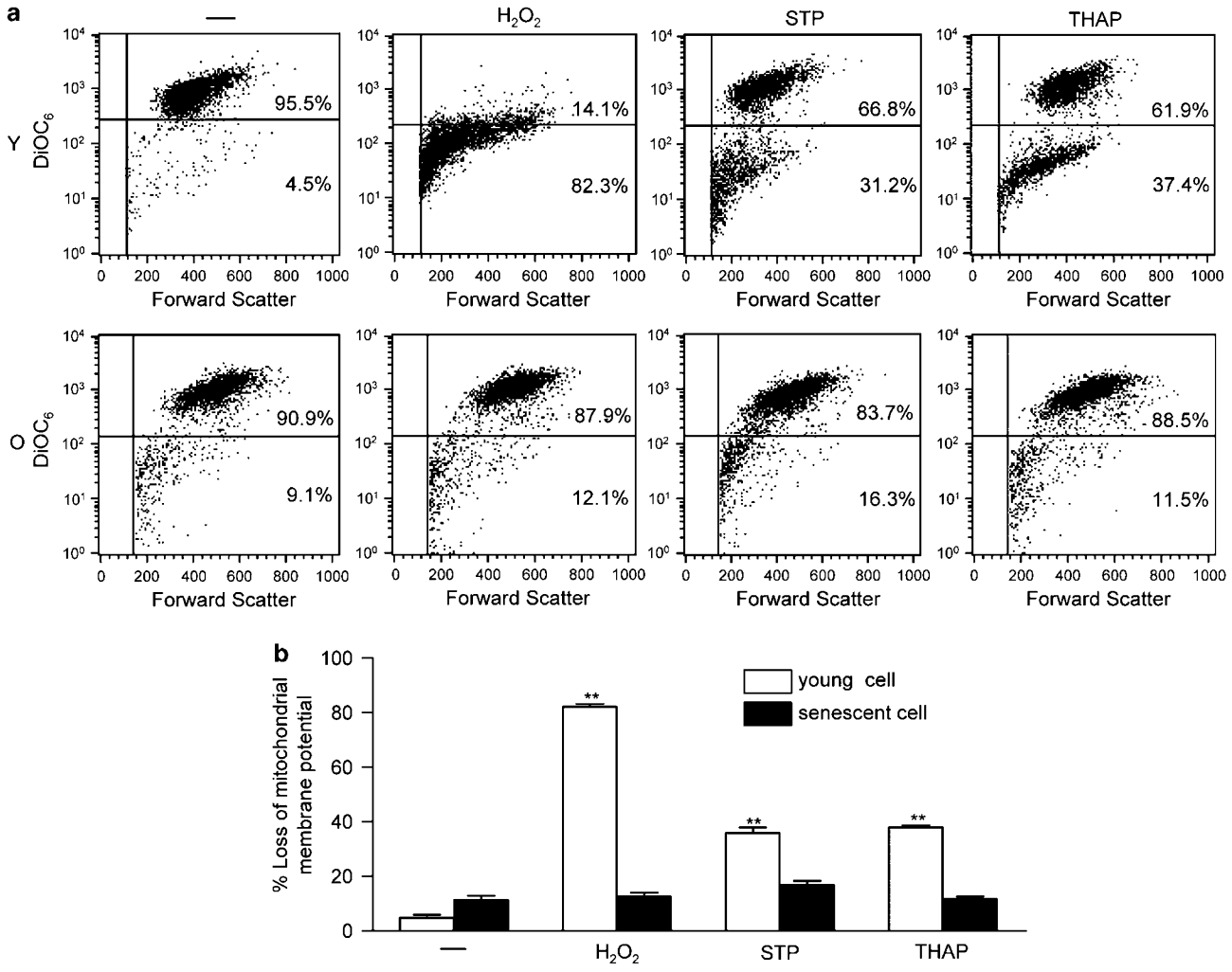

Figure 2 Mitochondrial membrane potential ($\Delta\Psi_m$) in H_2O_2, staurosporine or thapsigargin-treated young and senescent HDFs. (**a**) Young and senescent HDFs were treated with 1.5 mM H_2O_2, 100 nM staurosporine or 100 nM thapsigargin for 1, 3 and 48 h, respectively. The $\Delta\Psi_m$ was assessed by flow cytometry using $DiOC_6$ fluorescent staining, as described in Materials and Methods. Stress-induced changes in the young and senescent HDFs population distribution, according to $DiOC_6$ fluorescence, are shown as cytograms (abscissa: forward scatter; ordinate: $DiOC_6$ fluorescence). A distinct increase in the population of fibroblasts with a decrease in $\Delta\Psi_m$ is seen in the lower right quadrant, the upper right quadrant representing cells with high $\Delta\Psi_m$. (**b**) Quantitative graph of the change of mitochondrial membrane potential. The results shown are representative of three independent experiments; the histograms represent average and error bars represent standard deviations of the means. Significance was tested by ANOVA followed by a Dunnett post-test to compare the drug-treated group versus the control group. A double asterisk (**) denotes $P<0.01$. Y, young HDF cells; O, senescent HDF cells; STP, staurosporine; THAP, thapsigargin

with H_2O_2, staurosporine and thapsigargin. We observed that the basal expression levels of proapoptotic Bcl-2 family proteins such as Bak, Bik, Bok and Puma decreased in the senescent HDFs compared with young HDFs, whereas other Bcl-2 family proteins such as Bax and Bcl-x_L did not change (Supplementary Figure 1). The expression of Bcl-2 significantly increased in the senescent HDFs to 2.5-fold that of young HDFs (Figure 3a and b). Moreover, when HDF cells were treated with apoptotic stimuli (H_2O_2, staurosporine or thapsigargin), only young HDFs showed a reduction of Bcl-2 expression in contrast to senescent HDFs, which showed little or no change in the expression of Bcl-2 (Figure 3c). When we performed RT-PCR using specific Bcl-2 primer, Bcl-2 mRNA levels were downregulated in stress-induced apoptosis of young HDFs but not in senescent HDFs (Figure 3d), suggesting that the reduction of Bcl-2 occurs at the transcription level.

Role of Bcl-2 in apoptotic resistance of senescent HDFs. We downregulated Bcl-2 expression in senescent HDFs employing three different Bcl-2 siRNAs (no. 1, 2, and 3). A marked reduction of Bcl-2 protein as well as mRNA levels was evident 72 h after transfection of Bcl-2-specific siRNAs in senescent HDFs, compared to transfection of a control siRNA that had no effect (Figure 4a, b and c). When we downregulated Bcl-2 in senescent HDFs by transfecting with Bcl-2 siRNA no. 3, and examined their survival rates following treatment with 1.5 mM H_2O_2, 100 nM staurosporine or 100 nM thapsigargin for 24, 16 and 48 h, respectively, their survival rates were reduced after all the three treatments

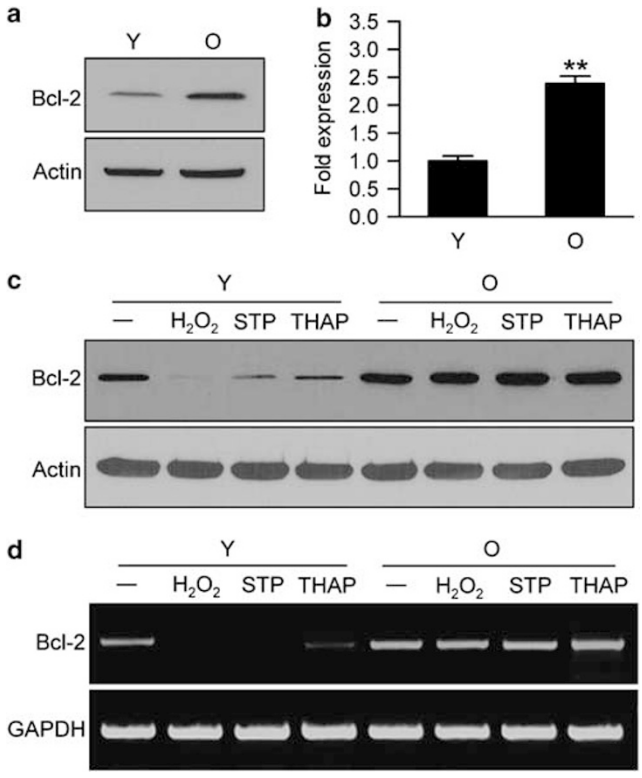

Figure 3 Failure of stress-induced Bcl-2 downregulation in senescent HDFs. (**a**) The expression level of Bcl-2 in young and senescent HDFs were determined by Western blotting using anti-Bcl-2 antibody. (**b**) Quantitative graph of Bcl-2. The results shown are representative of three independent experiments; the histograms represent average and error bars represent standard deviations of the means. A double asterisk (**) denotes $P<0.01$ in Student's *t*-test. Young and senescent HDFs were treated with 1.5 mM H_2O_2, 100 nM staurosporine or 100 nM thapsigargin for 12, 16 and 48 h, respectively. Cells were then harvested. Protein and mRNA expression level of Bcl-2 was determined by Western blotting using anti-Bcl-2 antibody (**c**) and RT-PCR using specific Bcl-2 primer (**d**). Actin and GAPDH are loading control. STP, staurosporine; THAP, thapsigargin; Y, young HDFs; O, senescent HDFs

(Figure 4d). As shown by fluorescence-activated cell sorter (FACS) analysis (Figure 4e and f) after treatment of the stress agonists, the subG_1/G_0 population increased by 25–30% in senescent HDFs transfected with Bcl-2 siRNA compared with those transfected with control siRNA. Also, in the Bcl-2 downregulated senescent HDFs, caspase-3 and PARP cleavages were markedly enhanced by staurosporine or thapsigargin treatments compared with those in control siRNA-transfected senescent HDFs (Figure 4g). In a previous study, we found that caspase-3 and PARP cleavages did not occur in H_2O_2-induced apoptosis of both young and senescent HDFs.[1]

Dysregulation of phospho-CREB in the senescent HDFs. CREB, a Bcl-2 transcription factor, plays a critical role in regulation of apoptosis in many cell types.[22,23] Phosphorylation of CREB on Ser-133 is associated with its increased transcriptional activity.[24] To investigate whether an increase in Bcl-2 level (Figure 3) correlates with phosphorylation of CREB, we checked phosphorylation status of CREB in H_2O_2, staurosporine or thapsigargin-treated young and senescent HDFs. As shown in Figure 5a, p-CREB (Ser-133) decreased in stress-induced apoptosis of young HDFs, in a time-dependent manner. Moreover, we found that young HDFs were more sensitive to the downregulation of p-CREB in staurosporine or H_2O_2-induced apoptosis compared with thapsigargin-induced apoptosis. However, p-CREB did not change in senescent HDFs after apoptotic stress (Figure 5b). In addition, we observed that the activity of other Bcl-2 transcription factors such as nuclear factor kappa B (NF-kB) and p53 did not change significantly in H_2O_2, staurosporine or thapsigargin-treated young and senescent HDFs (data not shown). To investigate whether CREB directly influences Bcl-2 levels, we reduced CREB levels in senescent HDFs using specific CREB-siRNA. As shown in Figures 5c and d, Bcl-2 was markedly reduced by the downregulation of CREB in CREB siRNA-transfected senescent HDFs but not in control siRNA-transfected senescent HDFs.

Protein phosphatase 2A (PP2A) is the primary enzyme that leads to dephosphorylation of p-CREB.[14] To investigate whether PP2A is involved in dephosphorylation of p-CREB in stress-induced apoptosis of young and senescent HDFs, we determined PP2A activities in young and senescent HDFs before and after agent treatments with H_2O_2, staurosporine and thapsigargin. As shown in Figure 6, apoptotic stimuli significantly increased PP2A activities only in young HDFs but not in senescent HDFs.

Discussion

Apoptosis plays an important role in many physiological and pathological processes, including aging and age-related diseases. One remarkable characteristic of the senescent phenotype is apoptotic resistance. How senescence develops apoptotic resistance is not clear. We focused on the role of Bcl-2 family proteins and their regulation for the resistance to apoptosis in senescent cells. A drop in mitochondrial membrane potential ($\Delta\Psi_m$) has been observed during early apoptosis induced by various apoptotic stimuli in many cell types.[25,26] It has been reported that some of the Bcl-2 family proteins, such as Bcl-2, Bcl-x_L and Bax, might directly modulate the $\Delta\Psi_m$[19,20] and the ratio of Bcl-2 to Bax determines whether a cell survives or dies following an apoptotic stimulus.[21] In this study, $\Delta\Psi_m$ did not change in senescent HDFs subjected to the apoptotic stress, whereas it was significantly reduced in young HDFs (Figure 2). In addition, we found that Bcl-x_L and Bax did not change in both young and senescent HDFs, but Bak, Bok, Bik and Puma decreased in senescent HDFs but not in young HDFs in contrast. (Supplementary Figure 1). Although several studies suggest that $\Delta\Psi_m$ is reduced in aged hepatocytes, fibroblasts, lymphocytes and cardiomyocytes,[16–18] the underlying molecular mechanism is not clear. Whether a decrease in Bak, Bok, Bik and Puma levels confers the decrease of $\Delta\Psi_m$ in senescent HDFs requires further study.

Since its discovery in the mid-1980s, proto-oncogene Bcl-2 has been shown to be a central player in mammalian cell death pathways.[8] Bcl-2 levels are reported to be high in follicular lymphoma, melanoma, and prostates and glioma

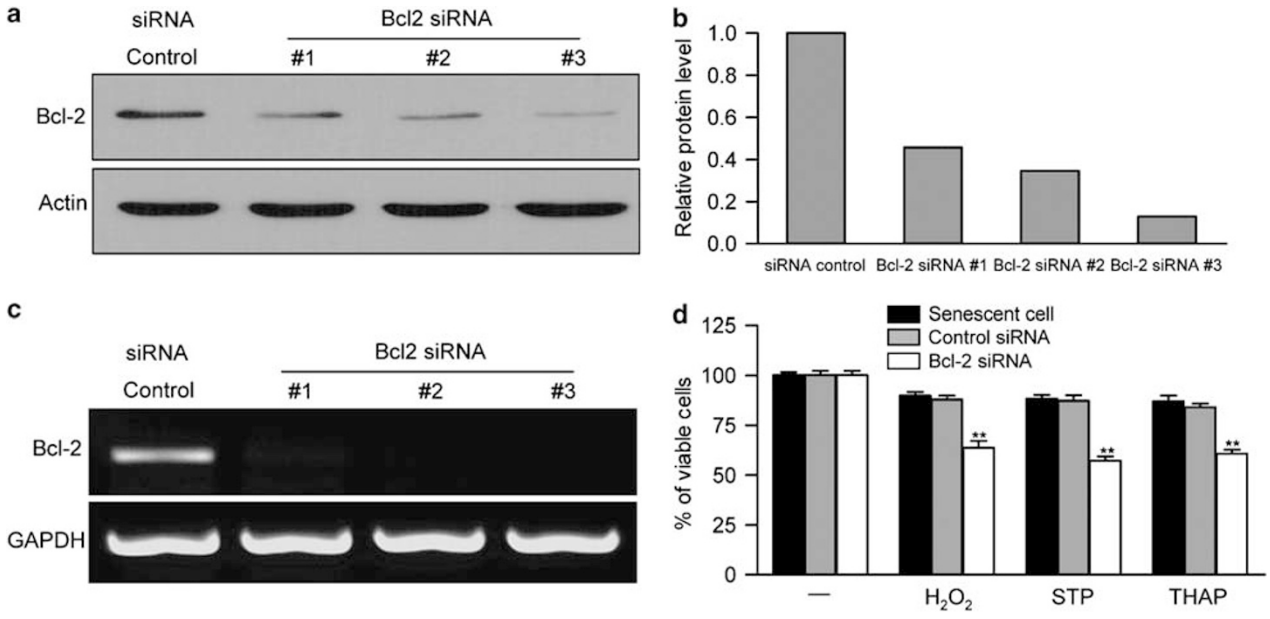

Figure 4 Role of Bcl-2 in apoptotic resistance in senescent HDFs. Senescent HDFs were transfected with three different siRNAs of Bcl-2 and control siRNA of GL2 luciferase, an siRNA directed against the firefly luciferase, using Oligofectamine. After 72 h, cells were harvested. Protein and mRNA expression of Bcl-2 were analyzed by Western blotting using anti-Bcl-2 antibody (**a**) and RT-PCR using Bcl-2 primer (**c**). (**b**) Quantitative graph of downregulated Bcl-2. (**d**) MTT assay. After transfecting Bcl-2-specific siRNA no. 3 for 72 h, cells were treated with 1.5 mM H_2O_2, 100 nM staurosporine or 100 nM thapsigargin for 24, 16 and 48 h, respectively. Error bars represent standard deviations of the means. (**e**) Senescent or control and Bcl-2 siRNA-transfected HDFs were treated with 1.5 mM H_2O_2, 100 nM staurosporine or 100 nM thapsigargin for 24, 16 and 48 h, respectively. Cells were harvested by trypsinization and then stained with PI. PI staining was determined by flow cytometry. (**f**) Quantitative graph of sub-G_1/G_O. The results shown are representative of three independent experiments; the histograms represent average and Error bars represent standard deviations of the means. (**g**) Senescent or control and Bcl-2 siRNA transfected HDFs were treated with 100 nM staurosporine or 100 nM thapsigargin for 16 and 48 h, respectively. Cells were harvested. PARP cleavage and caspase-3 activation were analyzed by Western blotting using anti-PARP or anti-caspase-3 antibodies. Significance was tested by ANOVA followed by a Dunnett post-test to compare the drug-treated group *versus* the control group. A double asterisk (**) denotes $P<0.01$. STP, staurosporine; THAP, thapsigargin; Y, young HDFs; O, senescent HDFs; Cont, control siRNA-treated senescent HDFs; Bcl-2, Bcl-2 siRNA-treated senescent HDFs

cancer cells.[27,28] We observed that Bcl-2 expression increased about 2.5-fold in senescent HDFs compared with young HDFs (Figure 3a and b). There have been several reports that apoptosis owing to external toxic stimuli can be rescued by Bcl-2.[29,30] As shown in Figures 3c and d, Bcl-2 protein and mRNA levels were downregulated by H_2O_2, staurosporine or thapsigargin treatments in the young HDFs but not in the senescent HDFs. Based on these findings, we hypothesized that the decrease in Bcl-2 sensitizes senescent HDFs to apoptotic stimuli and, conversely, increased levels of Bcl-2 in senescent cells makes them resist apoptotic stimuli. We confirmed this hypothesis by showing that downregulation of Bcl-2 in senescent HDFs, employing specific siRNA, resulted in the increased apoptotic sensitivity to stimuli such as H_2O_2, staurosporine and thapsigargin (Figure 4).

To understand why senescent HDFs contain higher levels of Bcl-2, we compared the levels of transcriptional factors for Bcl-2 genes in young and senescent HDFs, because a wide range of transcription factors, including CREB, Sp1, NF-kB, Myb and p53, have been shown to be involved in the regulation of Bcl-2 in different cell types.[31–34] As shown in Figure 5, p-CREB (Ser-133), which upregulates the transcription of Bcl-2, decreased after apoptotic stimuli in young HDFs but not in the senescent HDFs. There were no significant differences in the levels of other transcription factors for Bcl-2, such as NF-kB, Sp1 and p53, between the young and senescent HDFs subjected to the apoptotic stress (data not shown). Therefore, we focused on the regulatory role of p-CREB in age-related changes in Bcl-2. Downregulation of CREB by a specific siRNA caused the reduction in Bcl-2 (Figure 5c), which indicates an essential role of CREB for Bcl-2 expression. In addition, as the phosphorylation status of p-CREB on Ser-133 regulates the expression of Bcl-2, we compared PP2A activity in young and senescent HDFs after apoptotic stress. This enzyme is involved in inactivating CREB transcriptional activity by dephosphorylation of p-CREB.[15,16] Several recent studies have reported that activity of PP2A can be enhanced by the proapoptotic lipid ceramide and etoposide.[35] However, we found that PP2A activities significantly increased in young HDFs but not in the senescent HDFs after apoptotic stimuli (Figure 6). This indicates that increased activity of PP2A may possibly downregulate the Bcl-2 gene via dephosphorylation of p-CREB (Ser-133) only in the young HDFs. The reasons for these age-dependent changes in PP2A are not clear. It has recently been reported that PP2A activity is regulated by methylation of catalytic subunit and oxidation of cysteine residues in PP2A in the senescent HDFs.[35,36] Moreover, age-dependent increase of caveolin might suppress PP2A activity by their interaction.[37] Which of these mechanisms are operating dominantly in the senescent cells remains to be clarified.

In summary, senescent HDFs in contrast with young HDFs resist apoptosis, induced by three distinct stimuli: H_2O_2,

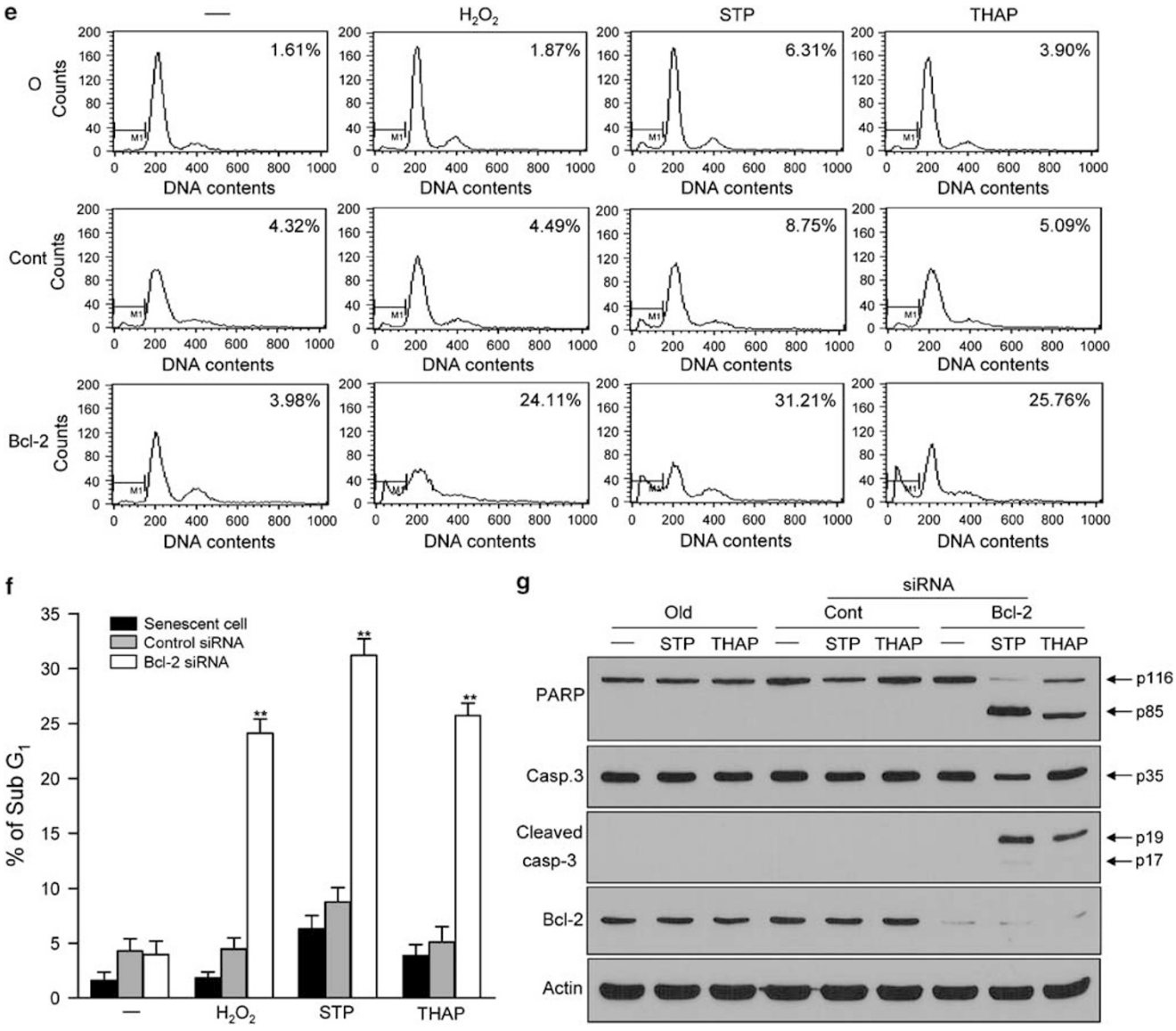

Figure 4 *Continued*

staurosporine and thapsigargin. This apoptotic resistance of senescent HDFs appears to be the result of failure of stress-induced downregulation of Bcl-2, which occurs in young HDFs.

Materials and Methods

Reagents. HDFs were isolated from human foreskins. Monoclonal antibody against actin (A5441) was purchased from Santa Cruz Biotechnology Inc. Polyclonal antibodies against PARP (9542), Caspase-3 (9662), Bcl-2 (2872), and p-CREB (9198) were purchased from Cell Signaling Technologies Inc. Staurosporine (569397) was from Calbiochem (La Jolla, CA, USA). Hydrogen peroxide (216763), thapsigargin (T9033), propidium iodide, and MTT were from Sigma Chemical Co (St. Louis, MO, USA). $DiOC_6$ (3,3′-diethyloxacarbocyanine) was from Molecular Probes. Ser/Thr Phosphatase Assay Kit 1 (17-127) was from Upstate Biotechnology Inc. Secondary horseradish peroxidase-conjugated antirabbit and antimouse antibodies were purchased from Zymed Laboratories Inc., and chemiluminescent detection systems were purchased from Pierce. All other biochemical reagents were from Sigma or Invitrogen.

Cell culture and treatment. The primary culture of normal HDF was isolated from the foreskin of a 4-year-old boy. HDFs were kept in 100 mm tissue culture dishes in Dulbecco's modified Eagle's medium, supplemented with 10% fetal bovine serum (FBS), 100 μ/ml penicillin, and 100 μg/ml streptomycin, maintained in 5% CO_2 in a humid incubator at 37°C. Cells were split serially *in vitro*. Young HDFs were frozen until old HDFs were generated through increased passages. Young proliferating cells and old near-senescent cells were collected at the doubling time of 24 h and over 2 weeks, respectively. Cellular senescence was confirmed using a senescence-associated (SA) β-galactosidase activity assay. HDFs were grown to 70% confluence and then treated with 1.5 mM H_2O_2, 100 nM staurosporine or 200 nM thapsigargin in serum-free media for the times indicated in Results.

Measurement of mitochondrial membrane potential ($\Delta\Psi_m$). Measurement of mitochondrial membrane potential was performed as described previously.[38] Briefly, HDFs were plated at a density of 3×10^5 (young cells) or 5×10^4 (senescent cells) on 100 mm culture plates. After treatment with H_2O_2, staurosporine and thapsigargin, respectively, for the times indicated in results, the cells were harvested by trypsinization, washed with culture medium and incubated with 80 nM $DiOC_6$ (3,3′-diethyloxacarbocyanine; Molecular probes) for 30 min in

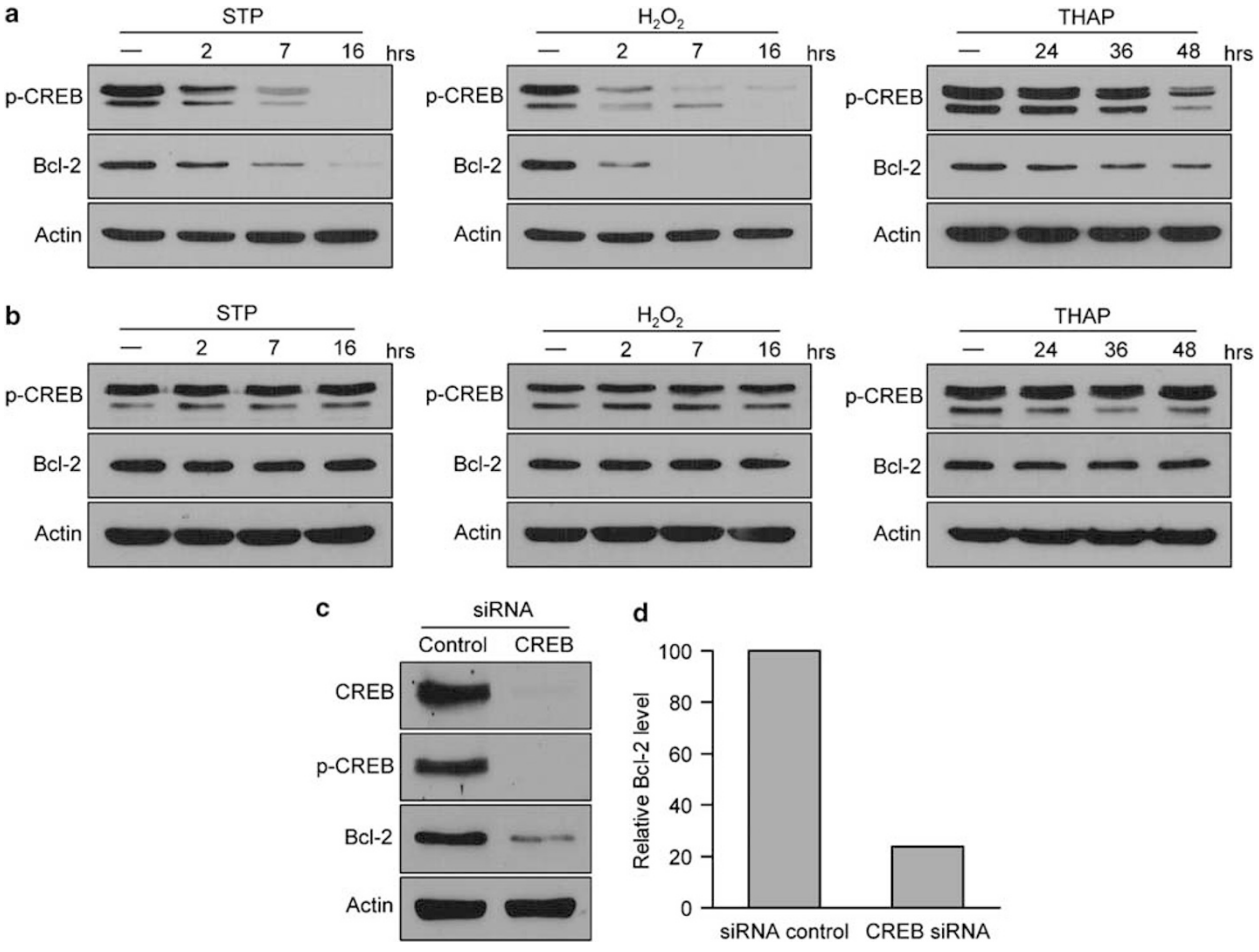

Figure 5 Expression of p-CREB (Ser-133) in H_2O_2, staurosporine or thapsigargin-treated young and senescent HDFs. Following 100 nM staurosporine, 1.5 mM H_2O_2 or 100 nM thapsigargin-treated young (**a**) and senescent HDFs (**b**) for indicated times, the cells were then harvested. (**c**) senescent HDFs were transfected with two different siRNAs of CREB and control siRNA of GL2 luciferase using Oligofectamine. After 72 h, cells were harvested. (**d**) the quantitative graph of downregulated Bcl-2. Immunoblot analyses were performed using CREB, p-CREB (Ser-133) and Bcl-2-specific antibodies. The blots were reprobed with antibody against actin to confirm equal protein loading. STP, staurosporine; THAP, thapsigargin

culture medium at 37°C. The cells were collected by centrifugation at 500 × g for 5 min, then resuspended in culture medium and analyzed immediately by flow cytometry with laser excitation at 488 nm. At least 10 000 events were recorded per sample. $DiOC_6$-stained cells were detected in channel FL1-H. Side scatter versus forward scatter served to gate on the cell population of interest, excluding debris. Data were obtained and analyzed with the CellQuest software on a Becton Dickinson FACScan. Error bars represent standard deviations of the means.

Analysis of apoptosis by cell cycle. Before treatment with H_2O_2, staurosporine and thapsigargin, cells were seeded in a 100 mm dish at 3×10^5 cells per dish. After treatments, the cells were harvested using trypsin–ethylenediamine-*N*,*N*,*N*′,*N*′-tetraacetic acid (EDTA), combined with floating cells collected from the medium, washed twice with PBS and fixed with ice-cold 70% ethanol. Cells were centrifuged and the ethanol supernatants discarded. The pelleted cells were then stained with 50 μg/ml propidium iodide (PI) plus RNase A for 20 min, and analyzed for DNA content on a FACScan flow cytometer (Becton Dickinson FACSorter) using CELLQuest software. Error bars represent standard deviations of the means.

Immunoblot analysis. Cells were lysed with lysis buffer containing 50 mM Tris pH 7.4, 150 mM NaCl, 1 mM EDTA pH 8.0, 1 mM protease inhibitor cocktail (Roche), 1 mM phenylmethylsulphonyl fluoride (PMSF), 1 mM NaF and 1 mM sodium orthovanadate. Protein contents were determined using Bradford assay. 40 μg protein of each sample was resolved by SDS-PAGE, transferred onto nitrocellulose membranes (Schleicher & Schuell Bioscience Inc) and blocked with TBS containing Tween-20 in 2.5% nonfat dry milk. The membranes were incubated with the primary antibodies at 4°C for 16 h. Secondary antibodies were added for 1 h at RT. The antibody-antigen complexes were detected using the ECL detection system (Pierce).

Semiquantitative RT-PCR. Total RNA was extracted from cultured HDFs using TRIZOL reagent (invitrogen), according to the manufacturer's protocol. Extracted RNA was treated with DNase I (Roche Diagnostics, Mannheim, Germany) and reverse transcribed to single-stranded cDNAs using oligo(dT) 12–18 primer with Superscript II reverse transcriptase (invitrogen). Appropriate dilutions of each single-stranded cDNA were prepared for subsequent PCR amplification by monitoring the actin gene as a quantitative control. Primer sequences were as follows:

5′-GGT GCC ACC TGT GGT CCA CCT G-3′ and 5′-CTT CAC TTG TGG CCC AGA TAG G-3′ for Bcl-2. 5′-CTG TGT GGA CTT GGG AGA GG-3′ and 5′-GGC ATC CAC GAA ACT ACC TT-3′ for GAPDH. RT-PCR was performed using the following conditions for Bcl-2 gene: 42°C for 1 h, 95°C for 15 min, 32 cycles of (i) 94°C for 30 s, (ii) 62°C for 30 min, (iii) 72°C for 1 min and 72°C for 10 min. Samples were analyzed by gel electrophoresis and bands were revealed by staining gels with ethidium bromide.

Protein phosphatase 2A activity assay. To determine the activity of PP2A, cells were washed twice with phosphate-free medium and lysed with a phosphatase extraction buffer containing 20 mM imidazole-HCl, 2 mM EGTA, 2 mM EDTA, pH 7.0, with protease inhibitor cocktail (Roche, 1 697 498), 1 mM PMSF, by sonication (Sonic Dismembrator 550, Fisher) twice at level 2 for 5 s. The whole

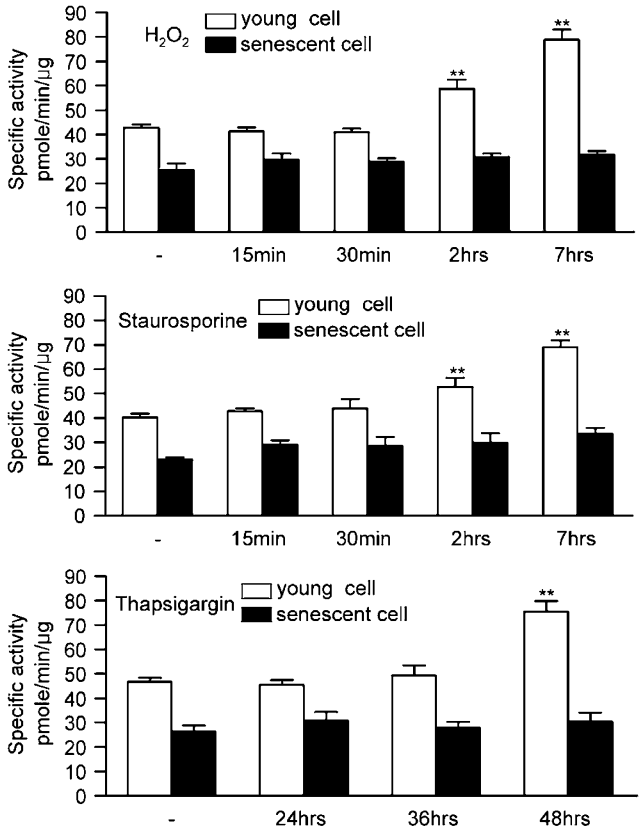

Figure 6 PP2A activity in H_2O_2, staurosporine or thapsigargin-treated young and senescent HDFs. Following 1.5 mM H_2O_2, 100 nM staurosporine or 100 nM thapsigargin-treated young and senescent HDFs for indicated times, the PP2A activity was assayed, as described in Materials and Methods. The results shown are representative of three independent experiments; the histograms represent average and error bars represent standard deviations of the means. Significance was tested by ANOVA followed by a Dunnett post-test to compare the drug-treated group at each time point versus the control group. A double asterisk (**) denotes $P<0.01$

lysates were centrifuged at 11 000 × *g* for 10 min, and the supernatants were used for the enzyme assay. Malachite Green Assay kit (Upstate Biotechnology, Lake Placid, NY, USA) was mixed with Thr(P) peptide (KRpTIRR, catalog number 12–219) purchased from Upstate Biotechnology Inc., as a substrate. An assay mixture (25 μl) containing 250 μM of substrate and 2 μg of each supernatant were incubated at 30°C for 10 min and then 100 μl of malachite green phosphate detection solution was. For color development, the assay mixture was incubated for 15 min at room temperature. To eliminate phosphate contamination arising from the cell extracts and the reagents, an assay mixture without the substrate or reagent was run. Phosphate released by the enzyme reaction was determined from the standard curve prepared with 0.1 mM potassium phosphate monobasic, KH_2PO_4. Absorbance of each well at 630 nm was read using a microplate reader (Benchmark, Bio-Rad).

RNA Interference and transfection. We targeted three regions of Bcl-2 mRNA and two regions of CREB mRNA for RNA interference. The target sequences were as follows: Bcl-2 #1: 5′-GGGAGGATTGTGGCCTTCTTTGAGT-3′; Bcl-2 #2: 5′-ACATCGCCCTGTGGATGACTGAGTA-3′; Bcl-2 #3: 5′-ACCTG CACACCTGGATCCAGGATAA-3′; CREB: 5′-ACAGCTGGCTAACAATGG-3′. A synthetic siRNA directed against the firefly luciferase mRNA sequence 5′-AACGUACGCGGAAUACUUCGA-3′ was used as a negative control. The siRNAs were purchased from Dharmacon Research (Lafayette, CO, USA) as duplexed 2'unprotected desalted and purified siRNAs. The transfection of siRNA duplexes was performed as described previously.[39] Briefly, senescent HDFs (5×10^4) were plated in a 100 mm dish, transfected with 0.5 nmole of siRNA and Oligofectamine™ reagent in serum-free medium and incubated for 4 h at 37°C in a CO_2 incubator. Following incubation, the cells were supplied with growth medium containing 10% fetal bovine seerum.

Acknowledgements. This work was generously supported by grants from the Aging and Apoptosis Research Center of KOSEF (R11-2002-097-05-001-0), the Korea Research Foundation for Health Science, and the SNU BK21 program from the Ministry of Education.

1. Ryu SJ, Cho KA, Oh YS, Park SC. Role of Src-specific phosphorylation site on focal adhesion kinase for senescence-associated apoptosis resistance. *Apoptosis* 2006; **11**: 303–313.
2. Cho KA, Ryu SJ, Oh YS, Park JH, Lee JW, Kim HP *et al.* Morphological adjustment of senescent cells by modulating caveolin-1 status. *J Biol Chem* 2004; **279**: 42270–42278.
3. Dimri GP, Lee X, Basile G, Acosta M, Scott G, Roskelley C *et al.* A biomarker that identifies senescent human cells in culture and in aging skin *in vivo*. *Proc Natl Acad Sci USA* 1995; **92**: 9363–9367.
4. Cho KA, Ryu SJ, Park JS, Jang IS, Ahn JS, Kim KT *et al.* Senescent phenotype can be reversed by reduction of caveolin status. *J Biol Chem* 2003; **278**: 27789–27795.
5. Seluanov A, Gorbunova V, Falcovitz A, Sigal A, Milyavsky M, Zurer I *et al.* Change of the death pathway in senescent human fibroblasts in response to DNA damage is caused by an inability to stabilize p53. *Mol Cell Biol* 2001; **21**: 1552–1564.
6. Yeo EJ, Hwang YC, Kang CM, Choy HE, Park SC. Reduction of UV-induced cell death in the human senescent fibroblasts. *Mol Cells* 2000; **10**: 415–422.
7. Pascal T, Debacq-Chainiaux F, Chretien A, Bastin C, Dabee AF, Bertholet V *et al.* Comparison of replicative senescence and stress-induced premature senescence combining differential display and low-density DNA arrays. *FEBS Lett* 2005; **579**: 3651–3659.
8. Cory S, Adams JM. The Bcl2 family: regulators of the cellular life-or-death switch. *Nat Rev Cancer* 2002; **2**: 647–656.
9. Wang E. Senescent human fibroblasts resist programmed cell death, and failure to suppress bcl2 is involved. *Cancer Res* 1995; **55**: 2284–2292.
10. Hardman RA, Afshari CA, Barrett JC. Involvement of mammalian MLH1 in the apoptotic response to peroxide-induced oxidative stress. *Cancer Res* 2001; **61**: 1392–1397.
11. Martin D, Salinas M, Fujita N, Tsuruo T, Cuadrado A. Ceramide and reactive oxygen species generated by H_2O_2 induce caspase-3-independent degradation of Akt/protein kinase B. *J Biol Chem* 2002; **277**: 42943–42952.
12. Tesauro M, Thompson WC, Moss J. Effect of staurosporine-induced apoptosis on endothelial nitric oxide synthase in transfected COS-7 cells and primary endothelial cells. *Cell Death Differ* 2006; **13**: 597–606.
13. Diaz-Horta O, Van Eylen F, Herchuelz A. Na/Ca exchanger overexpression induces endoplasmic reticulum stress, caspase-12 release, and apoptosis. *Ann NY Acad Sci* 2003; **1010**: 430–432.
14. Wadzinski BE, Wheat WH, Jaspers S, Peruski Jr LF, Lickteig RL, Johnson GL *et al.* Nuclear protein phosphatase 2A dephosphorylates protein kinase A-phosphorylated CREB and regulates CREB transcriptional stimulation. *Mol Cell Biol* 1993; **13**: 2822–2834.
15. Susin SA, Lorenzo HK, Zamzami N, Marzo I, Snow BE, Brothers GM *et al.* Molecular characterization of mitochondrial apoptosis-inducing factor. *Nature* 1999; **397**: 441–446.
16. Hagen TM, Yowe DL, Bartholomew JC, Wehr CM, Do KL, Park JY *et al.* Mitochondrial decay in hepatocytes from old rats: membrane potential declines, heterogeneity and oxidants increase. *Proc Natl Acad Sci USA* 1997; **94**: 3064–3069.
17. Martinez AO, Over D, Armstrong LS, Manzano L, Taylor R, Chambers J. Separation of two subpopulations of old human fibroblasts by mitochondria (rhodamine 123) fluorescence. *Growth Dev Aging* 1991; **55**: 185–191.
18. Rottenberg H, Wu S. Mitochondrial dysfunction in lymphocytes from old mice: enhanced activation of the permeability transition. *Biochem Biophys Res Commun* 1997; **240**: 68–74.
19. Marzo I, Brenner C, Zamzami N, Jurgensmeier JM, Susin SA, Vieira HL *et al.* Bax and adenine nucleotide translocator cooperate in the mitochondrial control of apoptosis. *Science* 1998; **281**: 2027–2031.
20. Shimizu S, Eguchi Y, Kamiike W, Waguri S, Uchiyama Y, Matsuda H *et al.* Bcl-2 blocks loss of mitochondrial membrane potential while ICE inhibitors act at a different step during inhibition of death induced by respiratory chain inhibitors. *Oncogene* 1996; **13**: 21–29.
21. Das A, Banik NL, Patel SJ, Ray SK. Dexamethasone protected human glioblastoma U87MG cells from temozolomide induced apoptosis by maintaining Bax:Bcl-2 ratio and preventing proteolytic activities. *Mol Cancer* 2004; **3**: 36.
22. Wilson BE, Mochon E, Boxer LM. Induction of bcl-2 expression by phosphorylated CREB proteins during B-cell activation and rescue from apoptosis. *Mol Cell Biol* 1996; **16**: 5546–5556.
23. Jambal P, Masterson S, Nesterova A, Bouchard R, Bergman B, Hutton JC *et al.* Cytokine-mediated down-regulation of the transcription factor cAMP-response element-binding protein in pancreatic beta-cells. *J Biol Chem* 2003; **278**: 23055–23065.
24. Gonzalez GA, Menzel P, Leonard J, Fischer WH, Montminy MR. Characterization of motifs which are critical for activity of the cyclic AMP-responsive transcription factor CREB. *Mol Cell Biol* 1991; **11**: 1306–1312.

25. Petit PX, Lecoeur H, Zorn E, Dauguet C, Mignotte B, Gougeon ML. Alterations in mitochondrial structure and function are early events of dexamethasone-induced thymocyte apoptosis. *J Cell Biol* 1995; **130**: 157–167.
26. Marchetti P, Susin SA, Decaudin D, Gamen S, Castedo M, Hirsch T *et al.* Apoptosis-associated derangement of mitochondrial function in cells lacking mitochondrial DNA. *Cancer Res* 1996; **56**: 2033–2038.
27. Gross A, McDonnell JM, Korsmeyer SJ. BCL-2 family members and the mitochondria in apoptosis. *Genes Dev* 1999; **13**: 1899–1911.
28. Weisenburger DD, Gascoyne RD, Bierman PJ, Shenkier T, Horsman DE, Lynch JC *et al.* Clinical significance of the t(14;18) and BCL2 overexpression in follicular large cell lymphoma. *Leuk Lymphoma* 2000; **36**: 513–523.
29. Chawla-Sarkar M, Bae SI, Reu FJ, Jacobs BS, Lindner DJ, Borden EC. Downregulation of Bcl-2, FLIP or IAPs (XIAP and survivin) by siRNAs sensitizes resistant melanoma cells to Apo2L/TRAIL-induced apoptosis. *Cell Death Differ* 2004; **11**: 915–923.
30. Lin CF, Chen CL, Chang WT, Jan MS, Hsu LJ, Wu RH *et al.* Bcl-2 rescues ceramide- and etoposide-induced mitochondrial apoptosis through blockage of caspase-2 activation. *J Biol Chem* 2005; **280**: 23758–23765.
31. Wilson BE, Mochon E, Boxer LM. Induction of bcl-2 expression by phosphorylated CREB proteins during B-cell activation and rescue from apoptosis. *Mol Cell Biol* 1996; **16**: 5546–5556.
32. Heckman CA, Mehew JW, Boxer LM. NF-kappaB activates Bcl-2 expression in t(14;18) lymphoma cells. *Oncogene* 2002; **21**: 3898–3908.
33. Frampton J, Ramqvist T, Graf T. v-Myb of E26 leukemia virus up-regulates bcl-2 and suppresses apoptosis in myeloid cells. *Genes Dev* 1996; **10**: 2720–2731.
34. Wu Y, Mehew JW, Heckman CA, Arcinas M, Boxer LM. Negative regulation of bcl-2 expression by p53 in hematopoietic cells. *Oncogene* 2001; **20**: 240–251.
35. Chen CL, Lin CF, Chiang CW, Jan MS, Lin YS. Lithium inhibits ceramide- and etoposide-induced protein phosphatase 2A methylation, Bcl-2 dephosphorylation, caspase-2 activation, and apoptosis. *Mol Pharmacol* 2006; **70**: 510–517.
36. Kim HS, Song MC, Kwak IH, Park TJ, Lim IK. Constitutive induction of p-Erk1/2 accompanied by reduced activities of protein phosphatases 1 and 2A and MKP3 due to reactive oxygen species during cellular senescence. *J Biol Chem* 2003; **278**: 37497–37510.
37. Li L, Ren CH, Tahir SA, Ren C, Thompson TC. Caveolin-1 maintains activated Akt in prostate cancer cells through scaffolding domain binding site interactions with and inhibition of serine/threonine protein phosphatases PP1 and PP2A. *Mol Cell Biol* 2003; **23** (24): 9389–9404.
38. Frank S, Oliver L, Lebreton-De Coster C, Moreau C, Lecabellec MT, Michel L *et al.* Infrared radiation affects the mitochondrial pathway of apoptosis in human fibroblasts. *J Invest Dermatol* 2004; **123**: 823–831.
39. Elbashir SM, Harborth J, Lendeckel W, Yalcin A, Weber K, Tuschl T. Duplexes of 21-nucleotide RNAs mediate RNA interference in cultured mammalian cells. *Nature* 2001; **411**: 494–498.

Supplementary Information accompanies the paper on Cell Death and Differentiation website (http://www.nature.com/cdd)